LAWRENCE
LIVERMORE
NATIONAL
LABORATORY

LLNL-JRNL-662218

Mechanism and Kinetic Modeling of Hydrogenation in The Organic Getter/Pd Catalyst/Activated Carbon Systems

L. N. Dinh, G. A. Cairns, R. Strickland, W. McLean II, R. S. Maxwell

October 8, 2014

Journal of Physical Chemistry A

Disclaimer

Mechanism and Kinetic Modeling of Hydrogenation in The Organic Getter/Pd Catalyst/Activated Carbon Systems

L. N. Dinh[1*], G. A. Cairns[2], R. A. Strickland[2], W. McLean II[1], R. S. Maxwell[1]

[1]Lawrence Livermore National Laboratory, Livermore, California, USA.

[2]AWE plc, Aldermaston, Reading, UK.

Keywords: hydrogen gettering, uptake kinetics

[*]Author to whom correspondence should be sent to (dinh1@llnl.gov)

Abstract

Experiments to measure the hydrogen uptake kinetics of DEB getter/Pd catalyst/activated carbon pellets have been performed under isothermal isobaric conditions. The extracted kinetics were then used to predict the performance of the getter pellets under different temperatures and pressures, including non-isobaric situations. For isothermal isobaric uptake at higher H_2 pressure (666.6-2666.5 Pa), H_2 solubility in the getter matrix is responsible for the uptake observed up to a 40-60% reacted fraction. Once the hydrogenated product becomes thicker, the diffusions of the reactants (atomic hydrogen and getter molecules) towards the reaction front become the rate limiting step. However, in a dynamic but very low H_2 pressure, encountered in many vacuum electronic applications, the hydrogen spillover effect, over micrometer scale, becomes the dominant reaction mechanism. Despite such a complex dependence of the rate limiting mechanisms on the experimental environment, there is good agreement between kinetic prediction models and experiments. The investigation also reveals that the ultimate uptake

capacity in the getter pellets scales inversely with the free volume of the vacuum vessel in which the DEB getter pellets are used, and that DEB getter pellets' performance greatly deteriorates during the final 10-15% capacity (as evidenced by the sharp bend in the slopes of the reacted fraction vs. time curves at 85-90% reacted fraction).

Introduction

Organic getters such as 1,4-bis(phenylethynyl)benzene (DEB), when blended with a carbon supported palladium catalyst to form pellets, have the ability to rapidly and irreversibly react with H_2. They also have a substantial capacity as each molecule of DEB is capable of storing 4 molecules of H_2. The proper use of such organic getters can prevent hydrogen gas accumulation in sealed containers, which may lead to hydrogen corrosion of materials, undesirable effects on electronic components, or an explosion hazard.[1-2] Currently, there are only a few published studies on the kinetics of the uptake of DEB pellets or DPB (1,4-diphenylbutadiyne) pellets and one paper on the ageing aspects of the DEB getter pellet.[3-7] All of the reported experimental works for DEB getter pellets were performed with uniquely designed experimental setups, which measured the hydrogen uptake under dynamic pressure conditions.[3-5,7] In addition to the scarcity of literature on the performances of these organic getter/Pd catalyst/ activated carbon systems, there is no comprehensive description of the dependence of the dominant uptake mechanism on the application environments.

In this report, for the first time, the hydrogen uptake measurement of DEB getter pellets was carried out in an isothermal isobaric environment. The uptake kinetics were then extracted to build kinetic models which can predict hydrogen uptake performances even under dynamic pressure environments. The level of agreement between predictive models and experiments, as

well as the implication that the rate limiting pathway is dependent upon the application environment, are then discussed.

Experimental setup and analysis methodology

Getter materials

The DEB getter pellets used in this work were manufactured by Honeywell Federal Manufacturing & Technologies at their Kansas City Plant and stored at room temperature (~294 K) in air until use in the experiments reported here. These pressed DEB pellets consist of 75 wt.% DEB and 25 wt.% catalyst (5 wt.% Pd on activated carbon) and have a microscopically porous structure to enhance the rate of hydrogen adsorption and subsequent reaction.[8] The DEB used in the pressed pellets was obtained from Kemex Laboratories with a purity of $\geq$ 99% and some trace amounts of impurities, the largest of which is H_2O. The activated carbon support (with a high surface area of 1100 m^2/g) serves to disperse the Pd catalyst throughout the DEB pellet structure. The Pd catalyst nanoparticles are thus randomly distributed throughout the DEB getter pellets to disassociate molecular hydrogen into atomic hydrogen. The atomic hydrogen is then added across the unsaturated carbon-carbon bonds in the DEB molecule, and its intermediates until fully hydrogenated, irreversibly storing the hydrogen in the C-H bond form. Without catalysts such as Pd or Pt, DEB cannot capture molecular hydrogen. The DEB pellets are cylinders with a diameter of approximately 2.85 mm and a height of 3.16 mm. Each pellet weights roughly 20.4 mg with a density of about 1.01 g/cm^3. The chemical structures of a virgin DEB molecule, a fully hydrogenated DEB molecule, and the optical image of some DEB getter pellets are shown in Fig.1.

Isothermal isobaric uptake experiments

Thermo-gravimetric approaches to the measurement of hydrogen uptake in organic getters are generally not accurate, since the hydrogenated by-products of the reaction tend to be volatile and cause weight loss in a weight gain experiment.[6] Unless the equilibrium vapor pressures of the hydrogenated species over their corresponding solids are known and therefore can be used to correct for the weight loss due to product volatility during thermo-gravimetric measurement of hydrogen uptake,[6] a technique based on hydrogen pressure drop is more preferable.

Fig. 2 shows a schematic diagram of the isothermal isobaric experimental setup reported in this manuscript. The setup consists of a bottle of research grade hydrogen connected to a 1925cc reservoir, a small 76.9cc reaction chamber which houses 20 DEB getter pellet for each experiment, and a MKS type 649A pressure controller which connects the reservoir chamber to the reaction chamber. During a typical isothermal isobaric experiment, 20 DEB getter pellets were placed in the reaction chamber, pumped to the high vacuum level, then heated to ~ 333 K overnight. This high vacuum annealing step has been reported to be sufficient to drive out adsorbed contaminants such as H_2O, CO, and CO_2, and to restore the maximum uptake capacity of air-exposed getter pellets to that of freshly made getter pellets.[7] The reaction chamber was then cooled under high vacuum (no exposure to any other gases except H_2 in the subsequent steps) to the desired reaction temperature (varying between 292-323K) which was kept to within ±0.5K difference between the reaction chamber and the reservoir chamber by commercial temperature controllers. During experiments, H_2 stored at pressures between 26000 to 47000 Pa in the reservoir was fed by the pressure controller into the reaction chamber to keep the pressure inside the reaction chamber (< 2667 Pa) constant. The pressure drop in the reservoir was directly

related to the hydrogen uptake by the pellets in the reaction chamber and recorded by a computer.

Constant rate of hydrogen injection experiments

In Fig. 3, a schematic diagram of the setup for a constant rate of hydrogen injection experiment is shown. Hydrogen is fed directly to a mass-flow controller which keeps the rate of hydrogen injection into the reaction chamber constant with time. In a typical constant rate injection experiment, the reaction chamber was first loaded with 25 DEB getter pellets, annealed at ~323K in a high vacuum overnight to get rid of adsorbed gases, and then cooled under vacuum to the reaction temperature. The plot in Fig. 4 illustrates the typical information provided by such experiments. Without getter in the reaction chamber, the hydrogen pressure curve in the chamber should rise linearly with time. However, when DEB getters are in the reaction chamber, they absorb hydrogen and keep the pressure in the reaction chamber low. After a while and when the getter pellets' remaining capacity is very low or completely used up, the pressure in the reaction chamber begins to rise linearly with the same slope as in the case without getter. The difference between the hydrogen pressure curves with and without getter corresponds to the amount of H_2 captured by the DEB pellets.

Isothermal model-fitting kinetic analysis

The rate equation for a general reaction can be written as:

$$\frac{d\alpha}{dt} = kf(\alpha) = \upsilon \exp\left(-\frac{E}{RT}\right) f(\alpha) \qquad (1)$$

where t is time; α is the reacted fraction (0 to 1); k is the rate constant; ν is the pre-exponential factor; E is the activation energy for the rate controlling process; R is the gas molar constant, T is

temperature in Kelvin; and $f(\alpha)$ is an analytical function determined by the rate-limiting reaction mechanism.

In the integral form:

$$g(\alpha) = \int_0^{\alpha} \frac{d\alpha}{f(\alpha)} = \upsilon . \exp\left(-\frac{E}{RT}\right) . t = k(T) . t \qquad (2)$$

A table listing possible rate limiting models with associated mathematical expressions for $f(\alpha)$ and $g(\alpha)$ is reproduced in Table I.[8] From eqn. (2), the most consistent (or probable) rate limiting model for the experimental data yields the best linear fit for the plot of g(α) vs. t. This is illustrated in the diagram of Fig. 5. The rate constant at a specific temperature T_i, $k(T_i)$, is obtained from the slope of the linear fit. Reaction kinetics can then be obtained using the Arrhenius equation in its logarithmic form at two or more different temperatures:

$$\ln\left[k(T_i)\right] = \ln(\upsilon) - \frac{E}{RT_i} \qquad (3)$$

Clearly, the slope of the linear fit for the plot of $ln[k(T_i)]$ vs. $1/T_i$ is simply $-E/R$ while the intercept is related to the pre-exponential factor, v. Once the kinetic parameters such as E and v are obtained and the most consistent rate limiting mechanism, $f(\alpha)$, is identified, a kinetic prediction of the reaction process as a function of temperature and time is possible through eqn. (1) and the proper $f(\alpha)$ expression from literature.[8]

Isothermal model-free kinetic analysis

However, if no linear fit can be obtained from eqn. (2) and the available $g(\alpha)$ expressions from literature,[8] then eqn. (1) can still be solved in a model-free approach very similar to that applied to the case of linear heating rate,[9-12] and will be described below:

Taking the natural logarithm on both sides of eqn. (1) yields:

$$\ln\left(\frac{d\alpha}{dt}\right) = -\frac{E}{RT} + \ln(vf[\alpha]) \tag{4}$$

At a specific value α_n for the isothermal experiment at T_i, eqn. (4) is more accurately written as:

$$\ln\left(\frac{d\alpha_n}{dt}\right) = -\frac{E_n}{RT_i} + \ln(\upsilon f[\alpha_n]) \tag{5}$$

If the experimenter performs more than 2 isothermal uptake experiments at more than 2 different temperatures, a plot of $\ln\left(\frac{d\alpha_n}{dt}\right) vs. 1/T_i$ has a slope $-E_n/R$ and an intercept equal to $\ln(vf[\alpha_n])$.

By repeating the above procedure at other α_n values between 0 and 1, a plot of E_n vs. α_n and a plot of $\ln(vf[\alpha_n])$ vs. α_n can be established. In other words, at every α_n value, a distinct pair of values for E_n and $vf(\alpha_n)$ is obtained from the Arrhenius plot built from all data at different temperatures with the same value of α_n, as pictorially illustrated in the diagram of Fig. 6.

Once the variations of E and $vf(\alpha)$ with respect to α are known, the time prediction, t_{α_n}, for a specific conversion α_n to be reached at any isothermal temperature T_o can be obtained from the rate equation (1) as following:

$$t_{\alpha_n} = \int_0^{t_\alpha} dt = \int_0^{\alpha} \frac{d\alpha}{\{\upsilon f(\alpha)\} e^{-\frac{E}{RT_o}}} \tag{6}$$

Results and Discussion

The plots of the reacted fractions vs. log(time) for the hydrogen uptake at a constant H_2 pressure of 1333.2 Pa for six isothermal experiments over a temperature range from 292.8K to 320.0K are presented in Fig. 7. The inset at the upper left corner of Fig. 7 is the zoomed up portion of the same curves at very low reacted fraction ($\alpha < 0.1$). It is observed that for the main portion of the reaction ($0.08 < \alpha < 0.94$), hydrogen uptake was faster with increasing temperatures, indicating a reaction with a positive activation energy barrier. However, at very low or very high reacted fractions ($\alpha < 0.08$ and $\alpha > 0.94$), there is no consistent trend. At $\alpha < 0.08$, some experiments at lower temperatures seem to go faster than those at higher temperatures. At $\alpha > 0.94$, some experiments reached almost 100% uptake capacity while other stalled at around 94%. The almost random differences in the uptake rates before 0.08% or after 94% getter capacity, as well as the different ultimate uptake capacities, were probably the result of a combination of variation in the samples' microstructures and some slight level of non-uniformity in the mixing of the pellets' constituents during synthesis. This slight non-uniform mixing could take the form of non-homogeneous distribution of Pd catalyst nanoparticles and/or deviation from the nominal composition of 75 wt.% DEB and 25 wt.% catalyst (5 wt.% Pd on activated carbon).

Attempts to apply the isothermal model fitting kinetic analysis described above with the data shown in Fig. 7 were not successful since none of the models listed in Table I yielded a satisfactory linear relationship between $g(\alpha)$ and t. The best fit with a linear relationship between $g(\alpha)$ and t for all temperatures is based upon the three dimensional diffusion model (D3). However, even the $g(\alpha)$ vs. t plots from the D3 model display a significant non-linear relationship as shown in Fig. 8. The hydrogenation process of the DEB pellets may be very complex, and the kinetics of the hydrogen uptake of the DEB pellets in the isothermal isobaric

environment may not be, therefore, accurately described by a single stage geometrical diffusion model.

Consideration of the hydrogen uptake process by DEB pellets at the atomic scale also leads to many questions and few answers (Fig. 9). The diagram on the right-hand side of Fig. 9 depicts an exploded view of a Pd catalyst inside a DEB pellet. Each hydrogen molecule is split into two hydrogen atoms upon adsorbing on the Pd catalyst surface. These hydrogen atoms react readily with DEB molecules that touch the surface of the Pd catalyst to form a product layer of hydrogenated DEB. After the formation of this product layer, between the Pd catalyst surface and virgin DEB, how does the reaction continue?

The Pd catalysts undoubtedly serve as local reservoirs for supplying hydrogen to surface sites. But would hydrogen leave the Pd catalyst surface and diffuse as atomic hydrogen on the activated carbon surface or through the thickening layer of hydrogenated DEB product to continue the reaction? Computationally, it has been argued that the energy barrier for hydrogen diffusion away from the Pd catalyst surface is prohibitive on graphene-like surfaces .[13] Hydrogen spillover is, nevertheless, a well-documented mechanism for heterogeneous catalytic reaction. It is described as dissociative adsorption of H_2 on metal catalyst particles, followed by migration of H atoms onto the support, and diffusion of H on the support (in most cases, graphite and activated carbon) to remote surface sites for reaction.[14-19] The average distance between Pd nano-particles in the DEB getter pellets is on the order of micrometers, but the maximum path length during which hydrogen atoms can diffuse on activated carbon or through hydrogenated DEB without recombination into H_2 molecules is currently not known. In general, the further the DEB molecules are from Pd catalyst sites, the less chance they have in reacting with hydrogen.

Isobaric uptake experiments at close to atmospheric pressure of hydrogen and fast dynamic uptake experiments such that the whole reaction completed in matters of 10-20 minutes produced a measureable temperature rise of 50-80K. However, the isothermal isobaric experiments reported here were carried out at < 2667 Pa and there was no temperature rise that could be experimentally detected by placing a thermocouple into the reacting DEB getter pellets. However, given the high mobility of DEB molecules as reported previously,[7] there was also an added possibility that a local temperature rise at the exothermic reaction front in addition to the applied heat induces microscopic diffusional transport of unreacted DEB molecules toward the catalyst surface to continue the reaction. This is not to mention that as the organic getter molecules become partially hydrogenated, they may not capture hydrogen as readily as their virgin counterparts.[6]

With such a multifaceted reaction mechanism, the hydrogen uptake kinetics in these porous DEB getter pellets may be more suitably extracted by the isothermal model-free kinetic analysis detailed in the previous section. In Fig. 10, the variation of the activation energy barrier and of $\ln(vf(\alpha))$, as obtained by the isothermal model-free kinetic analysis, were plotted as a function of the reacted fraction for isothermal isobaric uptake at 1333.2 Pa. The shaded bands drawn in the plots at $\alpha \geq 0.94$ are there to warn the readers that because of the variation in the pellets' microstructures and the slight level of non-uniformity in the mixing of the pellets' constituents during synthesis as discussed above, the accuracy in the values of E and $\ln(vf(\alpha))$ beyond $\alpha = 0.94$ is expected to sharply decrease.

In order to use the variation of E and $\ln(vf(\alpha))$ with respect to α in Fig. 10 to make kinetic predictions for the performance of DEB getter pellets at any pressure, p (other than P_{ref} = 1333.2 Pa), eqn. 1 can be rewritten with an explicit pressure dependence term of the form:[12]

$$\frac{d\alpha}{dt} = \upsilon \exp\left(-\frac{E}{RT}\right) f(\alpha) \left(\frac{P}{P_{ref}}\right)^n \tag{7}$$

There are a few possible values of n for the power of the pressure term in eqn. (7). If the mobile DEB molecules diffuse toward the Pd catalysts to capture H, the solubility of atomic hydrogen in the Pd catalyst is the main variable parameter in isobaric experiments performed at different pressures and is proportional to the square root of H_2 pressure (based on Sieverts' law) and n = ½ in eqn. (7). In the case of the atomic hydrogen diffusing away from the Pd catalyst surfaces onto the activated carbon surfaces, or through hydrogenated DEB as atomic hydrogen for micrometer scale distance, then the diffusion length can be written as:[6]

$$r = \sqrt{2DC_s \frac{m}{\rho} t} \tag{8}$$

where r is the diffusion length (in one, two, or three dimensional geometry), D is the diffusion coefficient, m is the mass of one hydrogen atom, ρ is the density of H in the product layer surrounding the Pd catalyst particles, and C_s is the concentration of H at the surface of the Pd catalyst which can be approximated with the solubility of H in Pd catalysts in an isobaric experiment. With this in mind, eqn. (8) becomes:

$$r = \sqrt{2D\left(KP_{H_2}^{1/2}\right)\frac{m}{\rho} t} \tag{9}$$

where K is the equilibrium constant in the Sieverts' law.

In short, n =1/4 if the hydrogen atoms leave the Pd surface onto the activated carbon surface or through hydrogenated DEB as atomic hydrogen to react with virgin DEB molecules some micrometer distance away. And finally, if the H_2 solubility in the surrounding DEB layer is the rate limiting step in the isobaric hydrogenation process, then it is possible that n = 1 if Henry's

law is applied. In short, for the hydrogen uptake in DEB getter pellets, the most likely values of *n* are ¼, ½, or 1.

In the top two plots of Fig. 11, the hydrogen uptake data (a) up to 80% hydrogenation and (b) after 80% hydrogenation from an isothermal isobaric experiment at 313.3K and 666.6 Pa (dark solid line) were plotted against the prediction models built from the kinetic parameters extracted from the 1333.2 Pa experiments and eqn. 7 with n = ¼ (light dashed line), with n = ½ (dark dashed line), and with n = 1 (light solid line). In the bottom two plots of Fig. 11, similar uptake data for another isothermal isobaric experiment at 313.3K and 2666.5 Pa are presented. Clearly, none of the prediction models perform superbly over the whole hydrogenation range. The model with n =1 fits better than the models with n = ½ and n = ¼ to a reactional fraction of α = 0.4 for the experimental curve at 666.6 Pa, but to a higher α value of 0.6 for the experimental curve at 2666.5 Pa. However, at higher α values, the fit with the experimental data from the models with n = ½ and ¼ gradually catch up and overtake the one from the model with n = 1, indicating a gradual switch in the rate limiting step for the hydrogen uptake reaction. Going beyond α = 0.8 and considering the uptake at 666.6 Pa, the model with n = ¼ fits a little better than the one with n = ½. This demonstrates the complex nature of the hydrogen uptake in DEB getter pellets.

The trend can be qualitatively interpreted as follows. Up to a conversion level of ~ 40-60%, it is the H_2 solubility in the DEB matrix that is responsible for the uptake obtained at different isobaric pressures. Once the hydrogenated product becomes thick (~ 40-60% hydrogenation), the diffusions of the reactants (atomic hydrogen or DEB molecules) toward the reaction front becomes the rate limiting step. It seems like at the latest stage of the isobaric reaction, when the product layer is thickest, the diffusion of atomic hydrogen away from Pd

surfaces toward the remaining DEB active sites (n = ¼) has a slight advantage over the movement of unreacted DEB molecules in the opposite direction (n = ½).

In Fig. 12, the predicted isothermal isobaric hydrogen uptake curves (dashed lines) at 313.3K with pressures of 666.6 Pa and 2666.5 Pa (obtained from the uptake kinetics shown in Fig. 10 and the use of eqn. (7) with n = 1 for lower α values (0.4 for the 666.6 Pa case and 0.6 for the 2666.5 Pa case, and n = ¼ for higher α values) are plotted together with the experimental curves (solid lines). The light shadows around the dashed lines represent a ± 5% error band around the prediction lines and suggest that, despite the disorderly trend near the reaction end, isothermal isobaric uptake at different temperatures and pressures can be approximated with the approach reported here. There is, however, a reduction in fidelity in the latest stage of the model resulting from the variation in the pellets' microstructures, the slight non-uniformity in the mixing of the pellets' constituents during synthesis and the possibility of a change in the reactivity of partially hydrogenated DEB, as previously postulated.

In reality, organic getters are often used as hydrogen scavengers in vacuum-sealed containers where zero or very low hydrogen partial pressure buildup over time are desired. In such applications, enough getter should be used to ensure very low H_2 partial pressure in the evacuated vessel, and the isobaric condition with high H_2 pressure to shorten experimental time and to facilitate kinetic analysis as described in the above section are absent. Under these conditions of dynamic but low partial H_2 pressure, the rate limiting step in the hydrogen uptake of the DEB getter pellets might not be the solubility of H_2 in the DEB matrix.

In Fig. 13, the hydrogen pressure buildup in a vacuum container (dark solid curve) with a volume of ~ 530cc, containing 25 DEB getter pellets, and subjected to a continuous injection of hydrogen at a rate of 2.3 μmol per min at 303K is plotted against prediction models employing

the kinetic parameters obtained from the isothermal isobaric experiments presented in Fig. 10 and eqn. (7) with n values of 1 (light solid curve), ½ (dark dashed curve), and ¼ (light dashed curve). In the prediction model for a non-isobaric process, a time step of Δt = 1 second was introduced into a Fortran programming code in order to use the reaction rate eqn. (7), which was written for an isothermal isobaric process. At the end of each Δt_i step, the H_2 partial pressure, P_i, in the vacuum container and the extent of reaction, α_i, was re-calculated and updated. During each Δt_i step, a pseudo-isobaric condition was assumed at α_i with P_i. Kinetic prediction modeling is also possible for non-linear H_2 input and/or non-constant situations provided that the input profile is known and the process is broken down into time steps of Δt_i, during which a pseudo-isothermal isobaric condition was assumed at α_i with P_i and T_i.

From Fig. 13, it is clear that the kinetic prediction model with n value of ¼ matches closest to the experimental data. This confirms that at very low but time-varying H_2 partial pressure, the rate limiting step in the hydrogen uptake is not the solubility of H_2 in the DEB matrix surrounding the Pd catalysts. Also at very low H_2 partial pressure, the exothermic reaction rate at the reaction front should be low enough not to drive up the local temperature around the reaction front, and as a result, unreacted DEB molecules do not have the necessary mobility to diffuse toward Pd surfaces to react with H atoms. Therefore, the hydrogen spillover effect, or the diffusion of hydrogen atoms away from the Pd catalyst sites on activated carbon or through the reacted product layer to react with fresh DEB molecules at micrometer scale distance away becomes the dominant reaction mechanism. Indeed, this process was witnessed throughout the temperature range of 295-323K under investigation and is illustrated by plotting the experimental H_2 pressure buildup curves vs. time (solid curves) and the kinetic prediction models with n = ¼ in Fig. 14. In Fig. 15, the "α vs. t" curves from the same experiments presented in

Fig. 14 (solid dark lines) are plotted against the ones from the kinetic prediction models (light dashed lines) with $n = ¼$. The shaded band around the prediction models represents a ± 5% error band. Clearly, some data shows better agreement than the others. Given the variations in the microstructures and constituents of the DEB getter pellets during the mixing phase of the synthesis which may affect not only the ultimate gettering capacity, but also the gettering rate, the results of the kinetic prediction modeling are good.

Note that in Fig. 14, the transition in the hydrogen pressure buildup curves in the reaction chambers from a horizontal line to a linear pressure rise with time signals the reacted fraction at which the performance of the DEB getter pellets drops significantly. This transition is seen in Figs. 12 and 15 as the sharp changes in slope of the α vs. t curves at around 85-90% consumption level, and is probably an indicator that, besides the increasingly more difficult transport of H to unreacted sites with a thicker product layer, it is chemically more difficult to saturate the DEB molecules with the last hydrogen bonds. As a result, the DEB getter pellets should be replaced at 85-90% consumption level in applications requiring low level of hydrogen partial pressure. Furthermore, due to the high volatilities associated with similar organic getters such as 1,4-diphenylbutadiyne (DPB) when partially hydrogenated,[7] partially hydrogenated products may vaporize at low temperatures and migrate away to unwanted regions of the vacuum container, resulting in lower total uptake capacity. In other words, when kept in a vacuum container with a smaller free volume, the ultimate uptake capacity of the getters is expected to be higher since the migration of partially hydrogenated product away from Pd catalyst sites in the DEB getter pellets is minimized. This is the very reason why, in this report, the total uptake capacities for the getter pellets in the isothermal isobaric experiments with a free volume of ~ 77cc are of the order of 94-100% (see Figs. 7, 11, and 12) while those for the getter pellets in the

constant rate of hydrogen input experiments with a free volume of ~ 530cc are all less than 94% (Fig. 15).

Since the volatility increases with increasing temperature, the application of the kinetic prediction modeling presented in this report should not be extended much beyond 323K. It is also possible that in the process of becoming fully hydrogenated, the activation energy barrier for capturing further H atoms from partially hydrogenated (or intermediate) DEB molecules may be very different than that for virgin DEB molecules. The interplay of this effect with the already complex nature of the hydrogenation of DEB getter pellets makes more accurate uptake hydrogen kinetic prediction by way of a specific model even more challenging. The description of such an effect is currently lacking in the literature and beyond the scope of this work.

Conclusion

Hydrogen uptake experiments have been performed with pellets of DEB/Pd /activated carbon in isothermal isobaric as well as in constant rate of H_2 injection modes. The model-free kinetic analysis has been successfully applied to the isothermal isobaric experiments to extract the hydrogen uptake kinetics, which were then used to make kinetic approximations for the performance of DEB getter pellets under different temperature and pressure schemes. The nature of the hydrogen uptake process in the organic getter/Pd catalyst/activated carbon systems is quite complex, with the rate limiting step verified to be different in the isothermal isobaric conditions under high pressures than in applications involving dynamic but low H_2 partial pressures.

For the first 40-60% of the reaction, H_2 solubility in the DEB getter matrix is the main differentiating factor for uptake under isothermal isobaric conditions at high hydrogen partial pressure. Thereafter, due to the thickening of the product layer between the Pd catalyst and

unreacted DEB molecules, the rate limiting step becomes the diffusion of the reactants (H atoms and DEB molecules). However, in an environment with very low H_2 partial pressure, the diffusion of hydrogen atoms away from the Pd catalyst sites to meet unreacted DEB molecules (or other organic getter) at remote locations becomes the dominant reaction mechanism. Hence, even though the hydrogen spillover effect is expected to be very weak in vacuum applications involving very low hydrogen partial pressure, it has been shown to be in operation. Such a complex dependence of the dominant uptake mechanism on the application environment should also be expected for the generic system of organic getter/ Pd catalyst/activated carbon system. Therefore, care must be taken to choose the proper rate limiting step for each application environment in order to have accurate kinetic prediction results.

Under all experimental conditions, it was observed that the ultimate uptake capacity of the DEB getter pellets scales inversely with the free volume of the vacuum vessel for which the DEB getter pellets are used. In addition, the H_2 uptake rate of the DEB getter pellets decreases by many orders of magnitude when the hydrogenated product layer is thick (after 85-90% consumption). This deterioration of the DEB getter's performance may allow gradual hydrogen accumulation. Depending on the rate of hydrogen generation in the vacuum system, DEB getter pellets have to be replaced upon saturation or even at 85-90% consumption level if a low hydrogen partial pressure in the vacuum vessel is to be maintained.

Acknowledgements

This work was performed under the auspices of the U.S. Department of Energy by Lawrence Livermore National Laboratory under Contract DE-AC52-07NA27344. Furthermore the authors express their gratitude to the useful discussion with Dr. P. Monks.

References

1. Yamanaka, S.; Sato, Y.; Ogawa, A.; Shirasu, Y.; Miyake, M. Poisoning Effect on Solubility of Hydrogen Isotopes in Getter Materials. *J. Nucl. Mater*. **1991,** *179*, 303-307.
2. Balooch, M.; Wang, Wei-E; Kirkpatrick, J. R. Hydrogen Uptake Mechanism of a Silicone-Rubber DEB Getter Mixture. *J. Polym. Sci., Part B: Polym. Phys.* **2001**, *39*,425-431.
3. Powell, G. L. Hydriding Kinetics of an Organic Hydrogen Getter-DPB. *J. Alloys Compd.* **2007,** *446-447*, 402-404.
4. Powell, G. L. Reaction of Hydrogen with a Hydrogen Organic Getter. *Advanced Materials for Energy Conversion II Symposium, The Materials Society Annual Meeting* **2004**, 257-261.
5. Powell, G. L. The Hydriding Kinetics of Organic Hydrogen Getters. *Advanced Materials for Energy Conversion II Symposium*, *The Materials Society Annual Meeting* **2004,** 467-475.
6. Dinh, L. N.; Schildbach, M. A.; Herberg, J. L.; Saab, A. P.; Weigle, J. C.; Chinn, S. C.; Maxwell, R. S.; McLean, W. II. Hydrogen Uptake of DPB Getter Pellets. *J. Nucl. Mater.* **2008,** *382*, 51-63.
7. Dinh, L. N.; Cairns, G. A.; Krueger, R.; Mayer, B. P.; Maxwell, R. S. Aging Aspects of DEB Getters. *J. Nucl. Mater.* **2013**, *442*, 298-305.
8. Galwey, A. K.; Brown, M. E. Thermal Decomposition of Ionic Solids; Elsevier: Amsterdam, The Netherlands, 1999.

9. Burnham, A. K.; Dinh, L. N. A Comparison of Isoconversional and Model-Fitting Approaches to Kinetic Parameter Estimation and Application Predictions. *J. Therm. Anal. Cal.* **2007,** *89*, 479-490.
10. Friedman, H. L. Kinetics of Thermal Degradation of Char-Forming Plastics from Thermogravimetry. Application to a Phenolic Plastic. *J. Polym. Sci., Part C: Polym. Lett.* **1964,** *6*,183-195.
11. Vyazovkin, S. Modification of The Integral Isoconversional Method to Account for Variation in The Activation Energy. *J. Comp. Chem.* **20*01**, *22*, 178-183.
12. Vyazovkin, S.; Burnham, A. K.; Criado, J. M.; Pérez-Maqueda, L. A.; Popescu, C.; Sbirrazzuoli, N. ICTAC Kinetics Committee Recommendations for Performing Kinetic Computations on Thermal Analysis Data. *Thermochim. Acta* **2011,** *520*, 1-19.
13. Maiti, A.; Dinh, L. N.; Baumann, T. F.; Maxwell, R. S.; Saab, A. P. Kinetics of Hydrogen Uptake by Scavenger Molecules – Insights from Molecular Modeling. *Chem. Phys. Lett.* **2009,** *475*, 223-226.
14. Weigle, J. C.; Phillips, J. Modeling Hydrogen Spillover in Dual-Bed Catalytic Reactors. *AIChE J.* **2004,** *50*, 821-828.
15. Su, F.; Lee, F. Y.; Lv, L.; Liu, J.; Tian, X. N.; Zhao, X. S. Sandwiched Ruthenium/Carbon Nanostructures for Highly Active Heterogeneous Hydrogenation. *Adv. Funct. Mater.* **2007,** *17*, 1926-1931.
16. Contescu, A. I.; Brown, C. M.; Liu, Y.; Bhat, V. V.; Gallego, N. C. Detection of Hydrogen Spillover in Palladium-Modified Activated Carbon Fibers During Hydrogen Adsorption. *J. Phys. Chem. C*, **2009,** *113*, 5886-5890.

17. Psofogiannakis, G. M.; Froudakis, G. E. DFT Study of The Hydrogen Spillover Mechanism on Pt-Doped Graphite, *J. Phys. Chem. C*, **2009,** *113*, 14908-14915.

18. Chen, L.; Cooper, A. C.; Pez, G. P. ; Cheng, H. Mechanistic Study on Hydrogen Spillover onto Graphitic Carbon Materials. *J. Phys. Chem. C,* **2007,** *111*, 18995-19000.

19. Hwang, S. W.; Rather, S. U.; Naik, M. U. D.; Soo, C. S.; Nahm, K. S. Hydrogen Uptake of Multiwalled Carbon Nanotubes Decorated with Pt–Pd Alloy Using Thermal Vapour Deposition Method. *J. Alloys Compd.,* **2009,** *480*, L20-L24.

Figure captions

Fig. 1: The chemical structures of a virgin DEB molecule, a fully hydrogenated DEB molecule, and the optical image of some DEB getter pellets.

Fig. 2: A schematic diagram of the isothermal isobaric experimental setup reported in this manuscript.

Fig. 3: A schematic diagram of the setup for a constant rate of hydrogen injection experiment.

Fig. 4: A diagram illustrating the type of information that can be provided by a constant rate of hydrogen injection experiments.

Table I: Possible rate limiting models with associated mathematical expressions for $f(\alpha)$ and $g(\alpha)$.

Fig. 5: For the isothermal model-fitting kinetic analysis, the most consistent rate limiting model yields the best linear fit to the plot of $g(\alpha)$ vs. t.

Fig. 6: For the isothermal model-free kinetic analyses, at every α_n value, a distinct pair of values for E_n and $vf(\alpha_n)$ is obtained from the Arrhenius plot built from all data at different temperatures with the same value of α_n.

Fig. 7: The plots of the reacted fractions vs. time for the hydrogen uptake at a constant H_2 pressure of 1333.2 Pa from 6 isothermal experiments with a temperature range from 292.8K to 320.0K. The inset at the upper left corner of Fig. 7 is the zoomed up portion of the same curves at very low reacted fraction ($\alpha < 0.1$).

Fig 8: The best fit with a linear relationship between $g(\alpha)$ and t for all temperatures is based upon the three dimensional diffusion model (D3). However, the $g(\alpha)$ vs. t plots from the D3 model still display a significant level of non-linearity.

Fig. 9: A diagram depicting the hydrogen uptake process by the DEB pellets at the atomic scale.

Fig. 10: The variation of the activation energy barrier, E, and of $\ln(vf(\alpha))$ as a function of the reacted fraction, α, as obtained by the isothermal isobaric model-free kinetic analysis are presented in (a) and (b), respectively.

Fig. 11: In the top two plots, the hydrogen uptake data up to 80% hydrogenation (a) and after 80% hydrogenation (b) from an isothermal isobaric experiment at 313.3K and 666.6 Pa (dark solid line) is plotted against the kinetic prediction models built from the kinetic parameters extracted from the 1333.2 Pa experiments and eqn. 7 with n = ¼ (lighter dashed line), with n = ½ (dark dashed line), and with n = 1 (light solid line). In (c) and (d), similar uptake data for another isothermal isobaric experiment at 313.3K and 2666.5 Pa are presented.

Fig. 12: The predicted isothermal isobaric hydrogen uptake curves (dashed lines) at 313.3K with pressures of 666.6 Pa (a) and 2666.5 Pa (b) are plotted together with the experimental curves (solid lines). The shaded band around the prediction models represents a ± 5% error bar.

Fig. 13: The hydrogen pressure buildup in a vacuum container (dark solid curve) with a volume of ~ 530cc, containing 25 DEB getter pellets, and subjected to a continuous injection of hydrogen at a rate of 2.3 μmol per min at 303K is plotted against prediction models with *n* values of 1 (light solid curve), ½ (dark dashed curve), and ¼ (light dashed curve).

Fig. 14: Comparisons of experimental H_2 pressure buildup curves vs. time (solid curves) and the kinetic prediction models with $n = ¼$ (dashed curves) at 295K (a), 303K (b), 308K, (c), 313K (d), 318K (e), and 323K (f).

Fig. 15: Comparisons of experimental "α vs. *t*" curves, from the same experiments presented in Fig. 14 (solid dark lines), with the kinetic predicted models utilizing $n = ¼$ (light dashed lines).

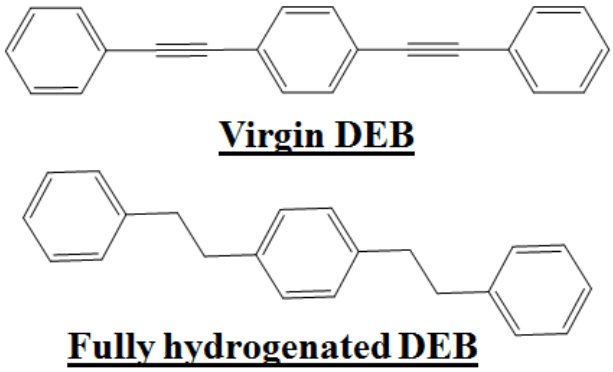

Virgin DEB

Fully hydrogenated DEB

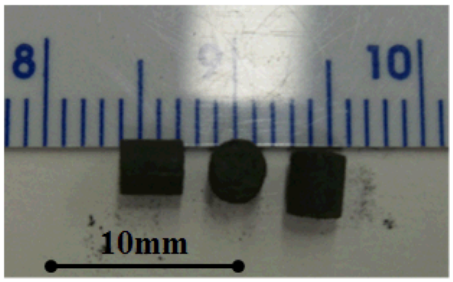

Pressed DEB getter pellets

Fig. 1

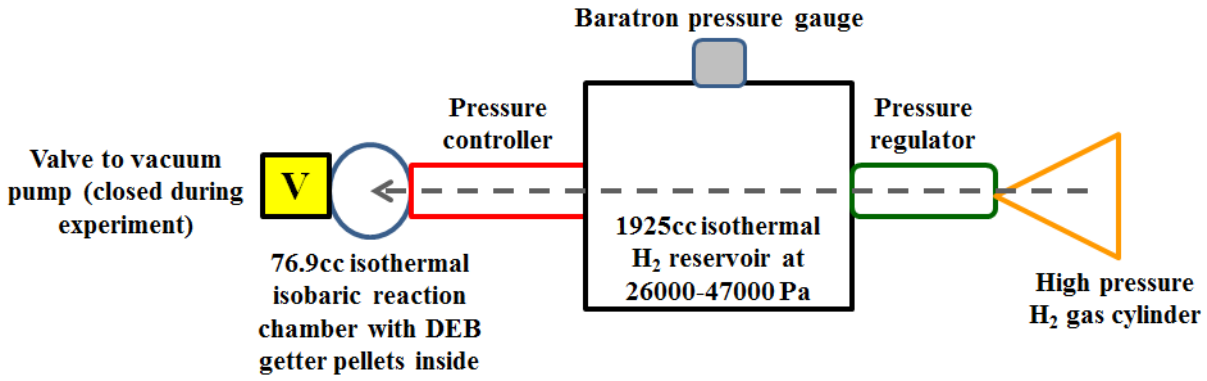
Baratron pressure gauge
Pressure controller
Pressure regulator
Valve to vacuum pump (closed during experiment)
V
1925cc isothermal H_2 reservoir at 26000-47000 Pa
76.9cc isothermal isobaric reaction chamber with DEB getter pellets inside
High pressure H_2 gas cylinder

Fig. 2

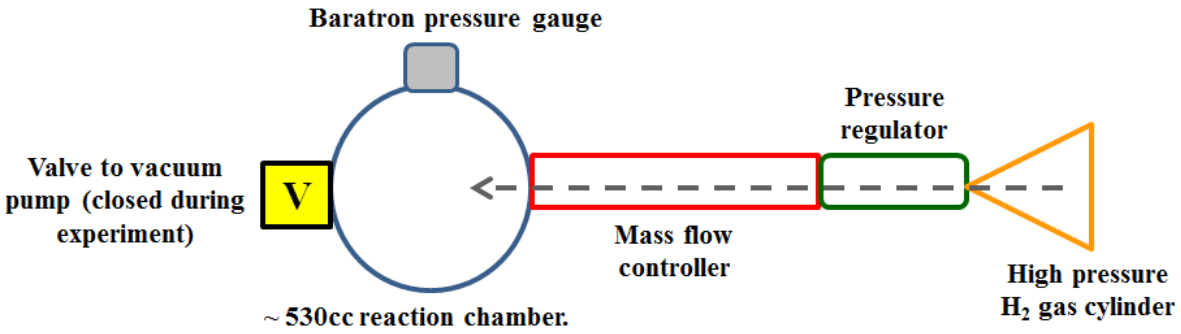
Baratron pressure gauge
Pressure regulator
Valve to vacuum pump (closed during experiment)
V
Mass flow controller
High pressure H_2 gas cylinder
~ 530cc reaction chamber.

Fig. 3

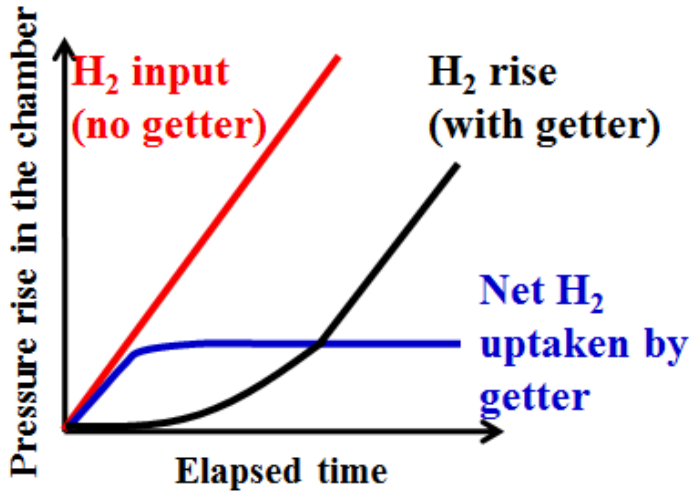
Pressure rise in the chamber
H2 input
(no getter)
H2 rise
(with getter)
Net H2
uptaken by
getter
Elapsed time

Fig. 4

Symbol	Rate determining mechanism	f(α)	g(α)
	Sigmoid *α-time*		
A2	Avrami-Erofeev	$2(1-\alpha)[-\ln(1-\alpha)]^{1/2}$	$[-\ln(1-\alpha)]^{1/2}$
A3	Avrami-Erofeev	$3(1-\alpha)[-\ln(1-\alpha)]^{2/3}$	$[-\ln(1-\alpha)]^{1/3}$
A4	Avrami-Erofeev	$4(1-\alpha)[-\ln(1-\alpha)]^{3/4}$	$[-\ln(1-\alpha)]^{1/4}$
B1	Prout-Tompkins	$\alpha(1-\alpha)$	$\ln[\alpha/(1-\alpha)]$
	Diffusion		
D1	1D diffusion	$1/2\,\alpha$	α^2
D2	2D diffusion (cylinder with no vol. change)	$[-\ln(1-\alpha)]^{-1}$	$(1-\alpha)\ln(1-\alpha)+\alpha$
D3	3D spherical diffusion (Jander)	$1.5(1-\alpha)^{2/3}[1-(1-\alpha)^{1/3}]^{-1}$	$[1-(1-\alpha)^{1/3}]^2$
D4	3D diffusion (Brounshtein-Ginstling)	$1.5[(1-\alpha)^{-1/3}-1]^{-1}$	$[1-2\,\alpha/3-(1-\alpha)^{2/3}]$
	Phase boundary movement		
R2	2D (cylindrical symmetry)	$2(1-\alpha)^{1/2}$	$[1-(1-\alpha)^{1/2}]$
R3	3D (spherical symmetry)	$3(1-\alpha)^{2/3}$	$[1-(1-\alpha)^{1/3}]$
	reaction order Law		
F0	zero order	1	α
F1	first order	$1-\alpha$	$-\ln(1-\alpha)$
F2	second order	$(1-\alpha)^2$	$[1/(1-\alpha)]^{-1}$
	Acceleratory *α*-time		
Pn	power law	$n(\alpha)^{(n-1)/n}$	$\alpha^{1/n}$
E1	exponential	α	$\ln\alpha$

Table I

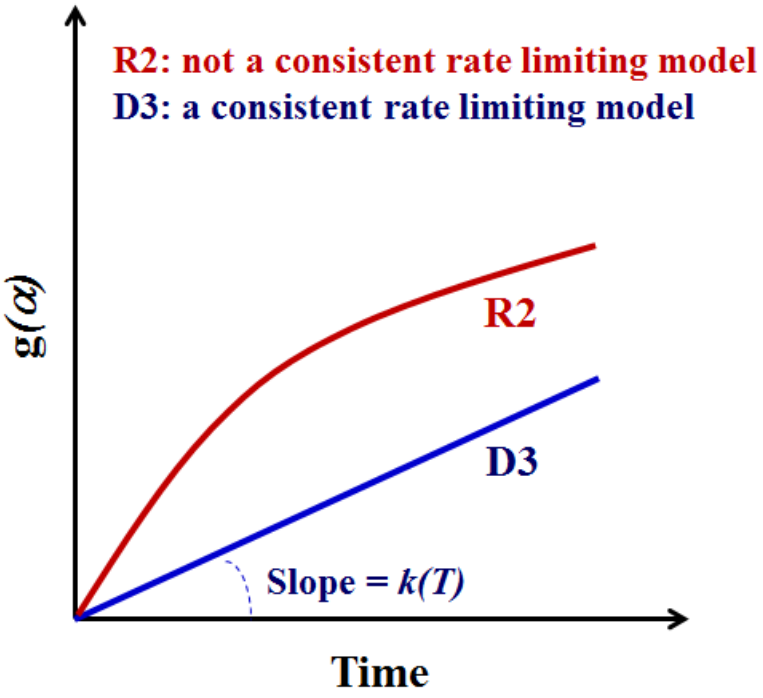
R2: not a consistent rate limiting model
D3: a consistent rate limiting model
g(α)
R2
D3
Slope = k(T)
Time

Fig. 5

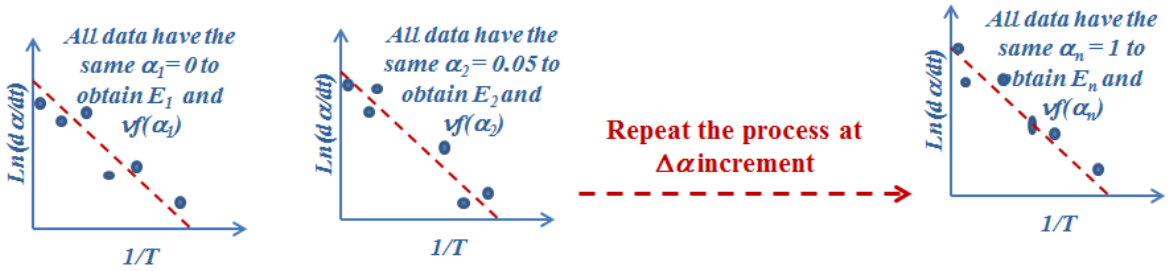
All data have the same α1= 0 to obtain E1 and vf(α1)
Ln(dα/dt)
1/T
All data have the same α2= 0.05 to obtain E2 and vf(α2)
Ln(dα/dt)
1/T
Repeat the process at Δα increment
All data have the same αn = 1 to obtain En and vf(αn)
Ln(dα/dt)
1/T

Fig. 6

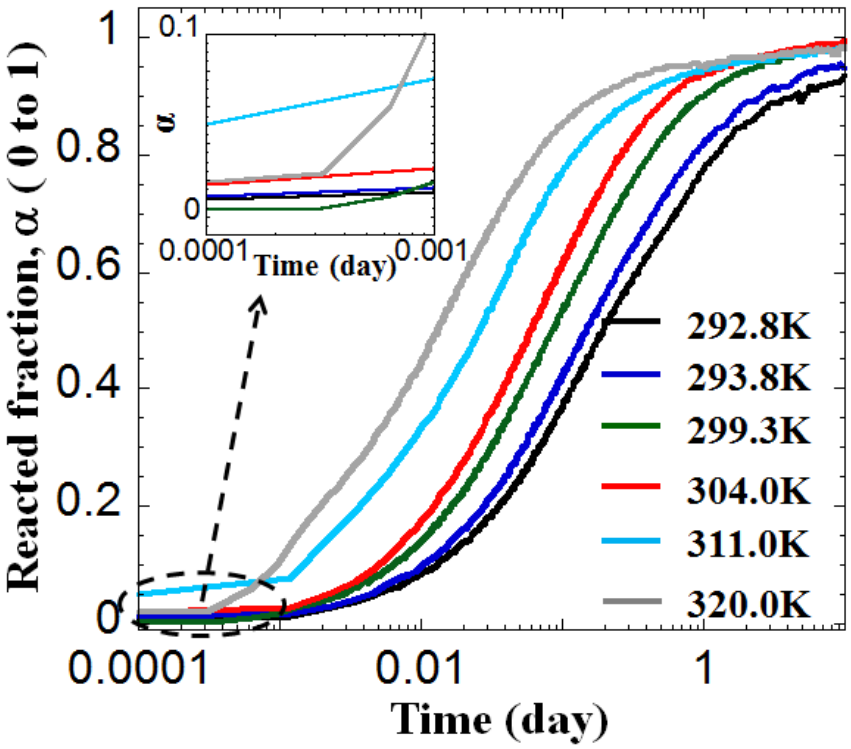
Reacted fraction, α (0 to 1)
Time (day)
0.0001
0.01
1
0
0.2
0.4
0.6
0.8
1
α
0.1
0
0.0001
0.001
Time (day)
292.8K
293.8K
299.3K
304.0K
311.0K
320.0K

Fig. 7

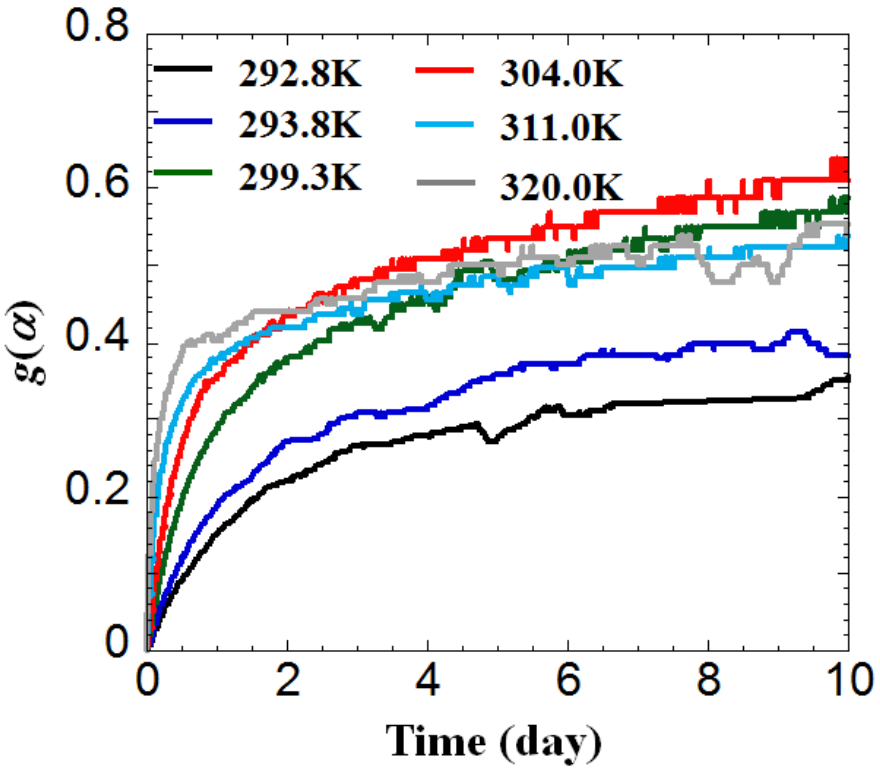
0.8
0.6
0.4
0.2
0
g(α)
0
2
4
6
8
10
Time (day)
292.8K
293.8K
299.3K
304.0K
311.0K
320.0K

Fig. 8

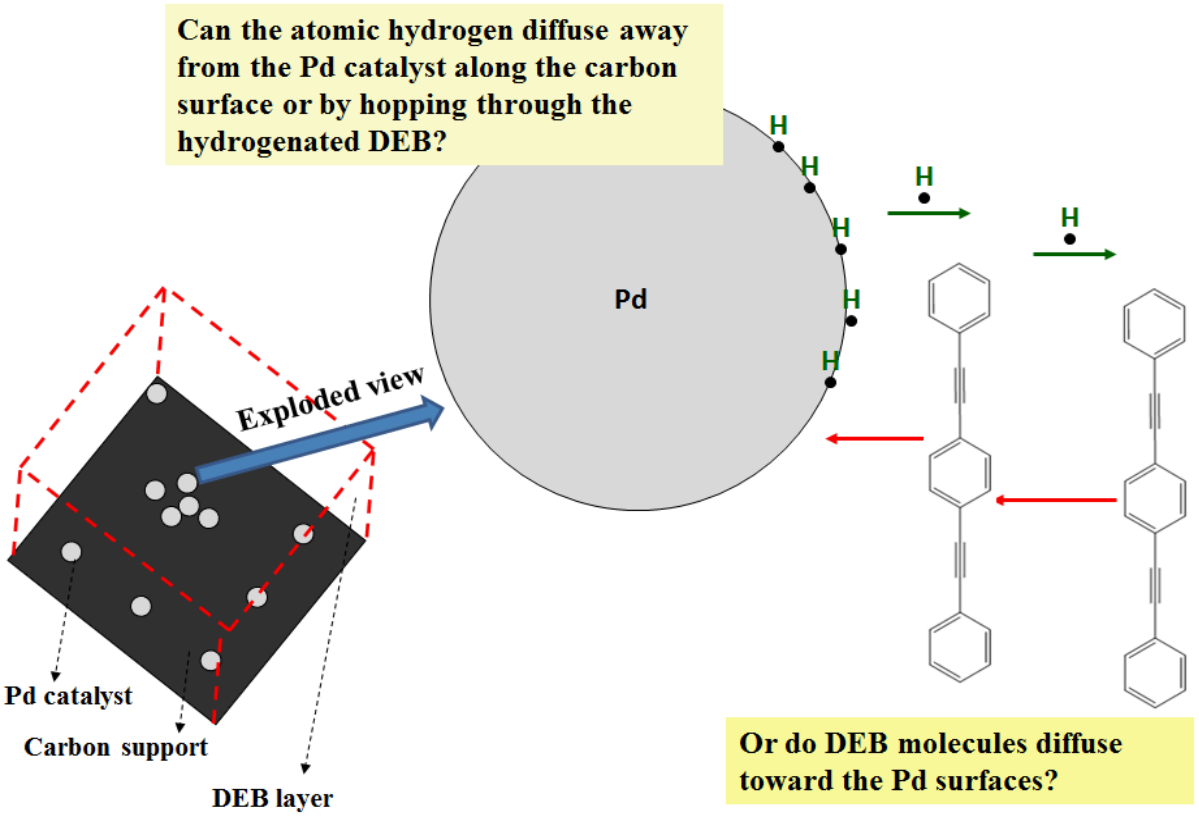
Can the atomic hydrogen diffuse away from the Pd catalyst along the carbon surface or by hopping through the hydrogenated DEB?
H
H
H
H
H
H
H
Pd
Exploded view
Pd catalyst
Carbon support
DEB layer
Or do DEB molecules diffuse toward the Pd surfaces?

Fig. 9

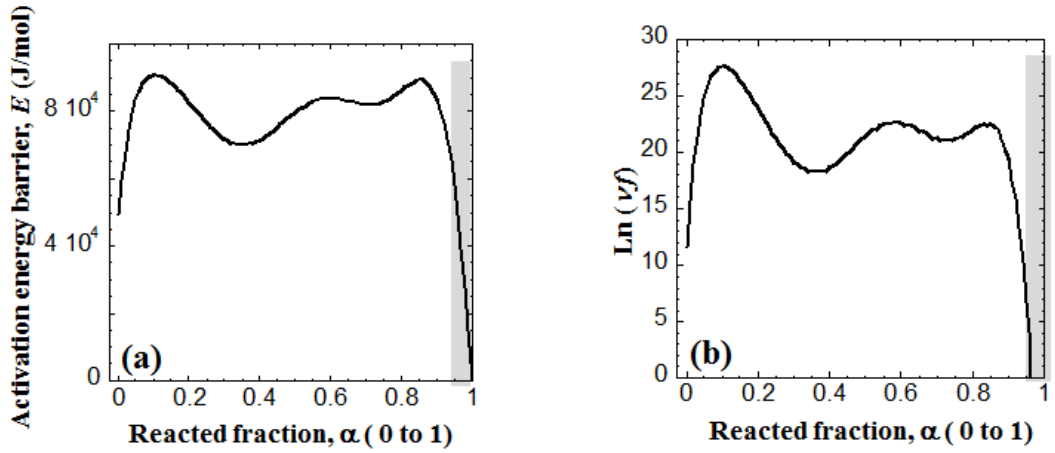
Activation energy barrier, E (J/mol)
8 10^4
4 10^4
0
(a)
0
0.2
0.4
0.6
0.8
1
Reacted fraction, α (0 to 1)
Ln (vf)
30
25
20
15
10
5
0
(b)
0
0.2
0.4
0.6
0.8
1
Reacted fraction, α (0 to 1)

Fig. 10

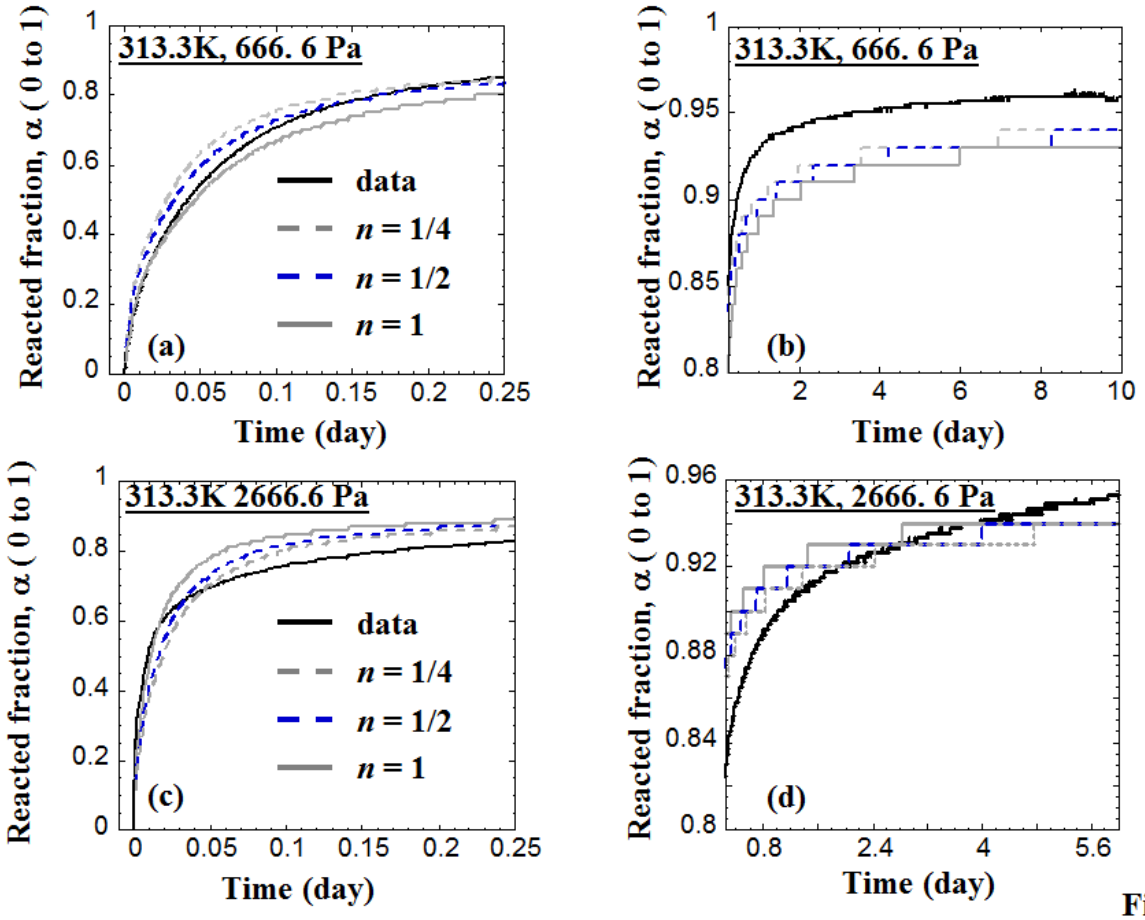
313.3K, 666. 6 Pa
Reacted fraction, α (0 to 1)
Time (day)
data
n = 1/4
n = 1/2
n = 1
(a)
313.3K, 666. 6 Pa
(b)
313.3K 2666.6 Pa
(c)
313.3K, 2666. 6 Pa
(d)

Fig. 11

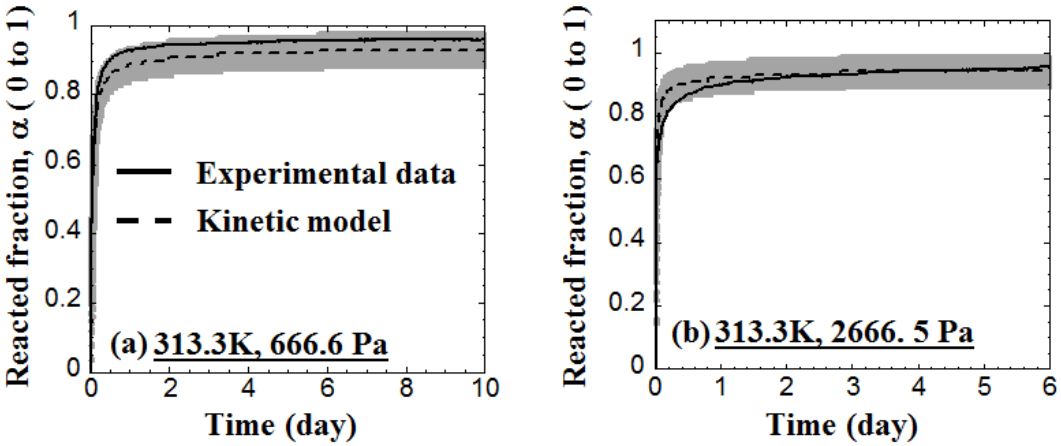
Reacted fraction, α (0 to 1)
Time (day)
Experimental data
Kinetic model
(a) 313.3K, 666.6 Pa
(b) 313.3K, 2666. 5 Pa

Fig. 12

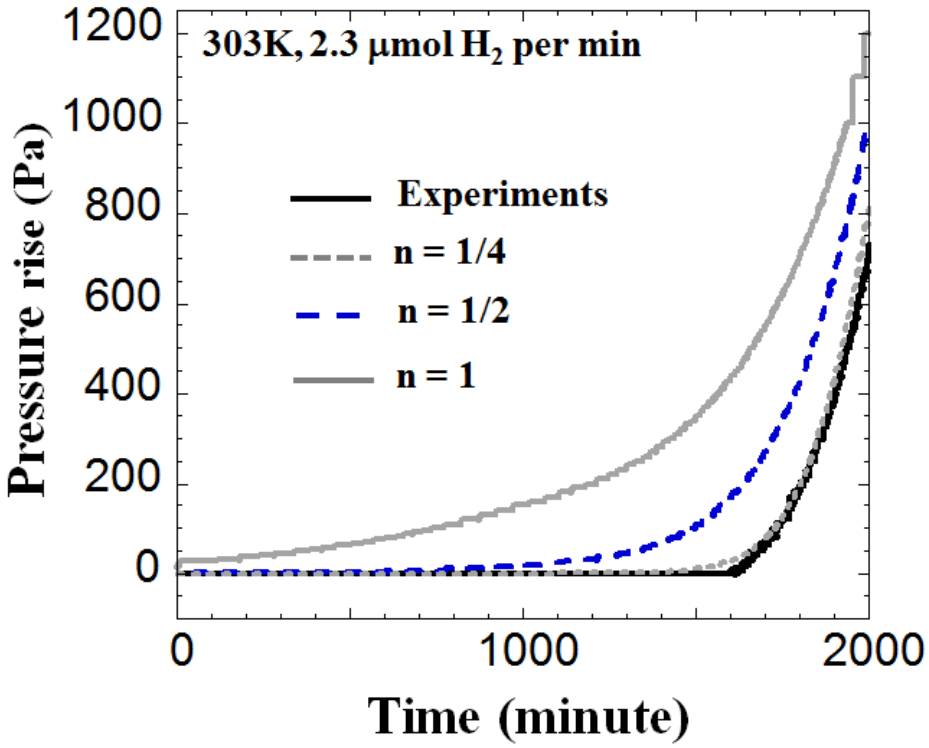
303K, 2.3 μmol H2 per min
Experiments
n = 1/4
n = 1/2
n = 1
Pressure rise (Pa)
Time (minute)
0
200
400
600
800
1000
1200
0
1000
2000

Fig. 13

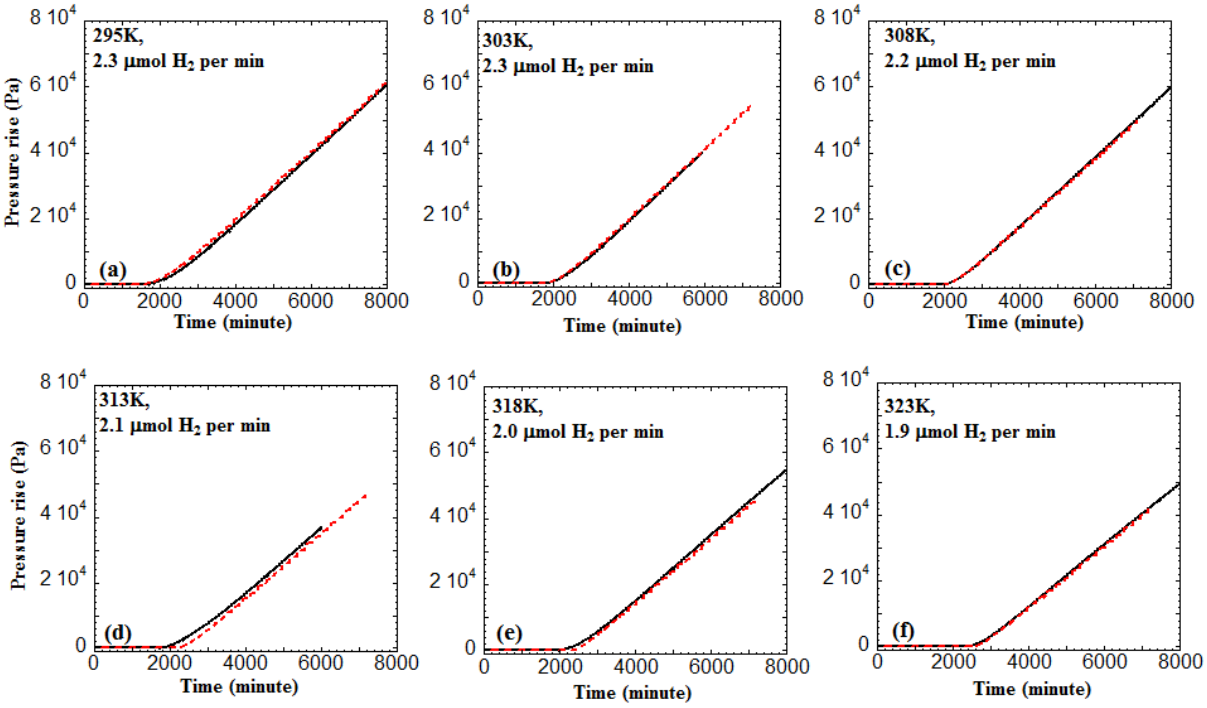
295K,
2.3 µmol H2 per min
(a)
303K,
2.3 µmol H2 per min
(b)
308K,
2.2 µmol H2 per min
(c)
313K,
2.1 µmol H2 per min
(d)
318K,
2.0 µmol H2 per min
(e)
323K,
1.9 µmol H2 per min
(f)
Pressure rise (Pa)
Time (minute)
8 10^4
6 10^4
4 10^4
2 10^4
0
2000
4000
6000
8000

Fig. 14

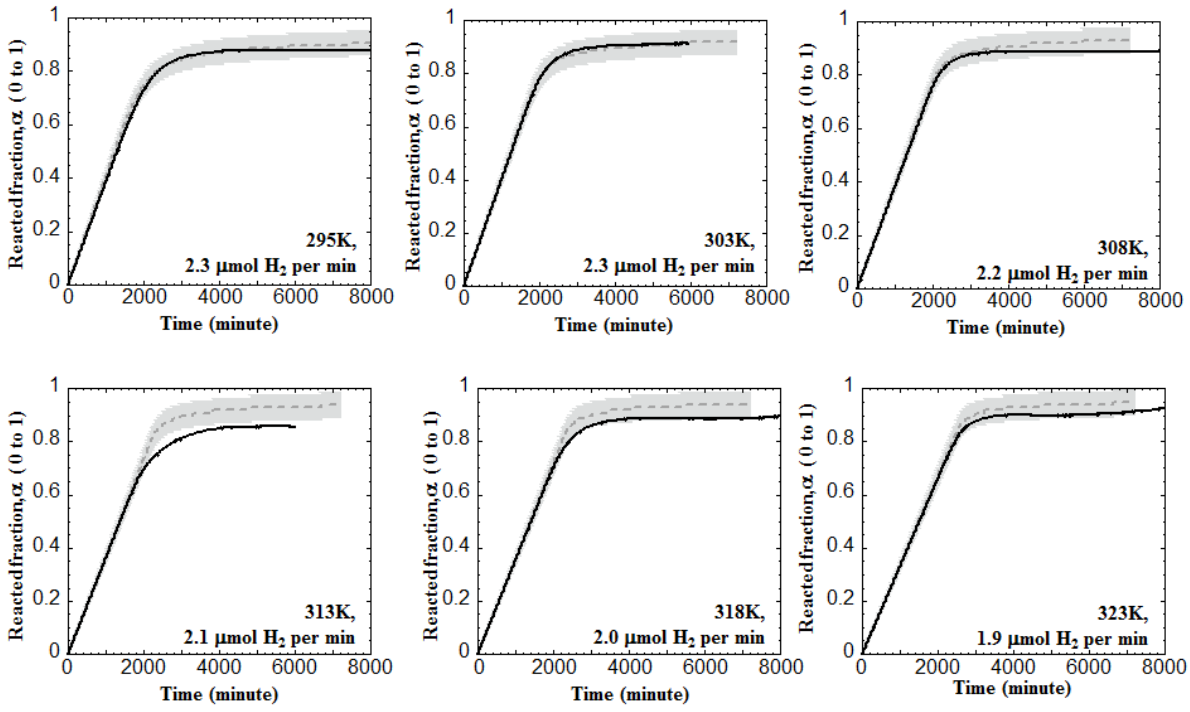
Reacted fraction, α (0 to 1)
Time (minute)
295K,
2.3 µmol H2 per min
303K,
2.3 µmol H2 per min
308K,
2.2 µmol H2 per min
313K,
2.1 µmol H2 per min
318K,
2.0 µmol H2 per min
323K,
1.9 µmol H2 per min

Fig. 15